

\mathbb{Z}_2 Gauge Field Coupled to a Fermion System

Jinyuan Wu

September 25, 2021

In the whole article we use σ and s as shorthands of σ^z and s^z , unless confusion may be caused by the notation.

1 The Model Hamiltonian

The model investigated in this article is shown in [5]. The model Hamiltonian is

$$H = H_Z - J \underbrace{\sum_{\langle i,j \rangle} \sigma_{ij} s_i s_j}_{H_{\text{Ising}}} + \sum_i h_i^x s_i^x - t \sum_{\langle i,j \rangle} \sigma_{ij} c_i^\dagger c_j, \quad (1)$$

where

$$H_Z = -g \sum_{l \in \square_{i^*}} \sigma_{ij}^z - h \sum_{\langle i,j \rangle} \sigma_{ij}^x, \quad (2)$$

where i^* is a site in the dual lattice (i.e. a site placed at the center of a plaquette), \square_{i^*} is the plaquette whose center is i^* , and l denotes a certain bond of a plaquette. Such kind of model Hamiltonian usually emerges from orthogonal metals [5, 6].

In this section, we introduce every part of (1).

1.1 \mathbb{Z}_2 Gauge Field and Its Dual Theories

1.1.1 The Plaquette Term

The plaquette term in the Hamiltonian of the \mathbb{Z}_2 gauge field is be a function of

$$F_{i^*} = \prod_{l \in \square_{i^*}} \sigma_l, \quad (3)$$

which is invariant under a \mathbb{Z}_2 gauge transformation

$$Q_i = \prod_{l \in +_i} \sigma_l^x. \quad (4)$$

A convenient convention is to let a plaquette share the same index with the site in its left bottom corner. An example of a \mathbb{Z}_2 gauge field configuration can be found in Figure 1 on page 1.

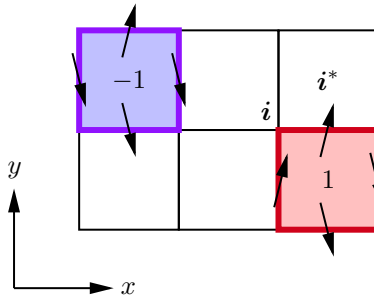


Figure 1: A \mathbb{Z}_2 gauge field configuration. The blue plaquette's F_{i^*} is $(-1) \times 1 \times (-1) \times (-1) = -1$, while the red plaquette's F_{i^*} is $1 \times 1 \times (-1) \times (-1) = 1$. Note that we assign the same index to a plaquette's center (labeled as i^* at the right top of the diagram) and the plaquette's left bottom site i . The terms “up” and “down” are defined in the Cartesian coordinates given in the diagram.

1.1.2 The Transverse Field

We name the \mathbb{Z}_2 gauge theory with plaquette terms only as the **Wegner model**, i.e.

$$H_W = -g \sum_i F_{i^*}. \quad (5)$$

There is no quantum fluctuation in H_W . The existence of interaction between the \mathbb{Z}_2 field and the Ising field and the fermions introduces effective interaction channels between \mathbb{Z}_2 excitations, but all effective interaction between \mathbb{Z}_2 excitations are in terms of σ_{ij}^z , which commutes with H_Z and therefore do not bring in quantum fluctuation.

An idiomatic way to add quantum fluctuation is to add a transverse field. In this project we consider a transverse field Hamiltonian in the form of

$$H_h = -h \sum_{\langle i,j \rangle} \sigma_{ij}^x, \quad (6)$$

where the parameter h measures the quantum fluctuation. (6) obviously commutes with Q_i for every i , so it can be a term in a \mathbb{Z}_2 gauge invariant Hamiltonian. In the language of string-net condensation, H_h is a string tension term. So when we say “ \mathbb{Z}_2 gauge theory”, usually we are referring to

$$H = -J \sum_i \prod_{l \in \square_{i^*}} \sigma_l - h \sum_{\langle i,j \rangle} \sigma_{ij}^x. \quad (7)$$

1.1.3 Equivalence between a \mathbb{Z}_2 Gauge Theory When $h = 0$ and a Bundle of Ising Chains

Now we consider a \mathbb{Z}_2 field theory with the plaquette term only, or in other words, we investigate the Wegner model. With the gauge choice

$$\sigma_{i, i+\hat{x}} = 1, \quad (8)$$

we have

$$F_{i^*} = \sigma_{i, i+\hat{y}} \sigma_{i+\hat{x}, i+\hat{x}+\hat{y}}, \quad (9)$$

which, by renaming $\sigma_{i, i+\hat{y}}$ into S_i , reads

$$F_{i^*} = S_i S_{i+\hat{x}}. \quad (10)$$

The hopping constant σ_{ij} , respectively, is

$$\sigma_{ij} = \begin{cases} 1, & j = i + \hat{x}, \\ S_i, & j = i + \hat{y}, \end{cases}, \quad \sigma_{ji} = \sigma_{ij}. \quad (11)$$

This, actually, means that the \mathbb{Z}_2 gauge field may also be transformed into a dual transverse field Ising field. For example consider Wegner model. With the definition of S_i it is rephrased into

$$H_W = -g \sum_i S_i S_{i+\hat{x}}, \quad (12)$$

so the model is actually a bundle of 1D Ising spin chain.

1.1.4 Mapping a \mathbb{Z}_2 Gauge Theory into a 2D Transverse Field Ising Model

$$H = -h \sum_{\langle I,J \rangle} \tau_I^z \tau_J^z - J \sum_I \tau_I^x. \quad (13)$$

(13) is often called the **dual transverse field Ising model** of \mathbb{Z}_2 gauge theory (7).

1.1.6 (Trivial) Deconfined Phase in Models with Long-range Interaction

If we are to extend the deconfined phase to $T > 0$, at least some stronger correlation must be introduced. Without introducing quantum fluctuation, a reasonable proposal may be

$$H_Z = - \sum_i \sum_{r=1}^{\infty} J(r) \prod_{a=0}^{r-1} F_{i^*+a\hat{x}},$$

or in terms of S_i s,

$$H_Z = - \sum_{r=1}^{\infty} J(r) \sum_i S_i S_{i+r\hat{x}},$$

which is again a bundle of spin chains without quantum fluctuation but this time with long range interaction. A famous example is the **Dyson-Ising chain**, which is defined as

$$H_Z = -g \sum_i S_i S_{i+\hat{x}} - J_r \sum_i \sum_r \frac{S_i S_{i+r\hat{x}}}{r^\omega}.$$

For 1D Ising chain with long-range interaction, there exists a thermal phase transition with zero transverse field, and indeed we get a deconfined phase with finite temperature, and as the temperature goes up the deconfined phase switches to the confined phase.

However, the so-called deconfined phase of a long-range interacting model is not of particular interest, because if you put manually something long-range into a model, *of course* it exhibits some long-range behaviors, for example Wilson loops obeying the perimeter law. That is why we call such a “deconfined phase” a trivial one. Despite its triviality, “deconfined” phases in long-range models give us a hint that strong interaction between \mathbb{Z}_2 fluxes is important for a thermal deconfined phase. A natural question to ask is, if we introduce more things into the model to induce effective interaction channels between \mathbb{Z}_2 fluxes, what happens when $T > 0$?

1.2 Orthogonal metals, emergent fermions and an Ising field

1.2.1 Fermion fractionalization in orthogonal metals and the effective model

Orthogonal metal is a type of fractionalized electron systems where an electron is split into another fermion and an Ising spin, i.e.

$$c_{i\alpha}^\dagger = f_{i\alpha}^\dagger \sigma_i^z, \quad (14)$$

where f operators and σ^z operators commute and $f_{i\alpha}^\dagger$ fermions can move around freely. Since the Hilbert space spanned by the f fermions and Ising spins are larger than the original electronic system’s Hilbert space, certain constraints must be imposed, resulting in an emergent gauge field, gluing up f and σ fields.

That justifies the way we construct (1). Suppose we have a tight-binding electron models with certain interaction channels that are strong enough to create a non-Fermi liquid phase, the Hamiltonian of which is

$$H = -t \sum_{\langle i,j \rangle, \alpha} c_{i\alpha}^\dagger c_{j\alpha} + \sum_{i,j} V_{ij} n_i n_j. \quad (15)$$

Substituting (14) into (15) and doing necessary mean field approximations, we find that the Hamiltonian about f fermions in the model is also a tight-binding Hamiltonian with its hopping constants being the same as σ_{ij} , which couples the fermions with the \mathbb{Z}_2 gauge field, endowing the fermions \mathbb{Z}_2 charges.

The idea of orthogonal metals gives us an approach to find a local \mathbb{Z}_2 gauge model that shows deconfined phase at finite temperature. Our logic is the inverse of the derivation of orthogonal metals: if an orthogonal metal with \mathbb{Z}_2 gauge structure does exist, then it can be described by (1). That implies the existence of a model Hamiltonian in the form of (1) with a deconfined phase. Our goal is, therefore, to check under what condition (1) *can never* be in a deconfined phase.

1.2.2 Confined phase in orthogonal metals

When the \mathbb{Z}_2 charges get trapped into a confined phase, it can be expected that the fermions and the Ising spins are also confined. Note that what the composite particles generated by the gauge field as a glue in the confined phase are is not quite clear. One possibility is that the fermions are glued together, forming something like Cooper pairs, where the fermion excitations are now gapped. Nonetheless, note that orthogonal metals are generated in a strongly correlated *electron* systems, so it is highly likely that *one fermion and one Ising spin* are glued together, restoring the electrons. In this case, the confined phase is just an ordinary metal, with gapless fermions (electrons). At high temperature \mathbb{Z}_2 excitations are confined (in the sense defined in Section 1.1.5), so (1) is just an ordinary metal.

2 Principles of Monte Carlo simulation: path integral, fermions and more

We are going to study (1) numerically. In the partition function, the (non-normalized) weight of a configuration is $\langle n | e^{-\beta H} | n \rangle$, given that $\{|n\rangle\}$ is a basis. We use a discrete path integral method to evaluate these weights.

We introduce a Trotter decomposition with imaginary time step $\Delta\tau = \beta/m$, choose σ_{ij}, s_i as labels for the \mathbb{Z}_2 field and the Ising field, respectively, and integrate out the fermion hopping term. Now a configuration of the systems is a sequence of length m , and at each imaginary time point τ there is a \mathbb{Z}_2 field $\sigma_{ij}(\tau)$ and an Ising field $s_{ij}(\tau)$. The weight of a configuration is

$$\begin{aligned} W(\sigma, s) &= \text{tr}_{\text{fermion}} \prod_{\tau=1}^{m\Delta\tau} \langle (\sigma, s)(\tau + \Delta\tau) | e^{-\Delta\tau H_Z} e^{-\Delta\tau H_{\text{Ising}}} | (\sigma, s)(\tau) \rangle e^{\Delta\tau \sum_{\langle i,j \rangle} \sigma_{ij}(\tau) c_i^\dagger c_j} \\ &= \prod_{\tau=1}^{m\Delta\tau} \langle (\sigma, s)(\tau + \Delta\tau) | e^{-\Delta\tau H_Z} e^{-\Delta\tau H_{\text{Ising}}} | (\sigma, s)(\tau) \rangle \det \left(1 + \prod_{\tau=1}^{m\Delta\tau} e^{\Delta\tau t \sigma(\tau)} \right) \\ &= \prod_{\tau=1}^{m\Delta\tau} \langle \sigma(\tau + \Delta\tau) | e^{-\Delta\tau H_Z} | \sigma(\tau) \rangle \langle s(\tau + \Delta\tau) | e^{-\Delta\tau H_{\text{Ising}}} | s(\tau) \rangle \det \left(1 + \prod_{\tau=1}^{m\Delta\tau} e^{\Delta\tau t \sigma(\tau)} \right). \end{aligned}$$

where $\sigma = \{\sigma_{ij}(\tau)\}$ and $s = \{s_i(\tau)\}$, and in the last line values of $\sigma(\tau)$ replaces the σ^z operators in H_{Ising} .

2.1 Path integral for 2D Transverse Field Ising Model

2.1.1 From 2D Transverse Field Ising Model to 3D Classical Ising Model

In this section we use σ to denote spin-1/2 degrees of freedom in a 2D transverse field Ising model. This notation conflicts with the symbol σ for \mathbb{Z}_2 gauge field, and is inconsistent with the symbol s for the Ising field, but since we do not deal with the complete (1) it does not matter. We also let $\sigma^z = \{\sigma_i^z(\tau)\}$ be the field configuration at τ .

The transverse field Ising model is

$$H_{\text{TFIM}} = -J \sum_{\langle i,j \rangle} \sigma_i^z \sigma_j^z + h \sum_i \sigma_i^x. \quad (16)$$

An imaginary time step in the path integral of (16) is

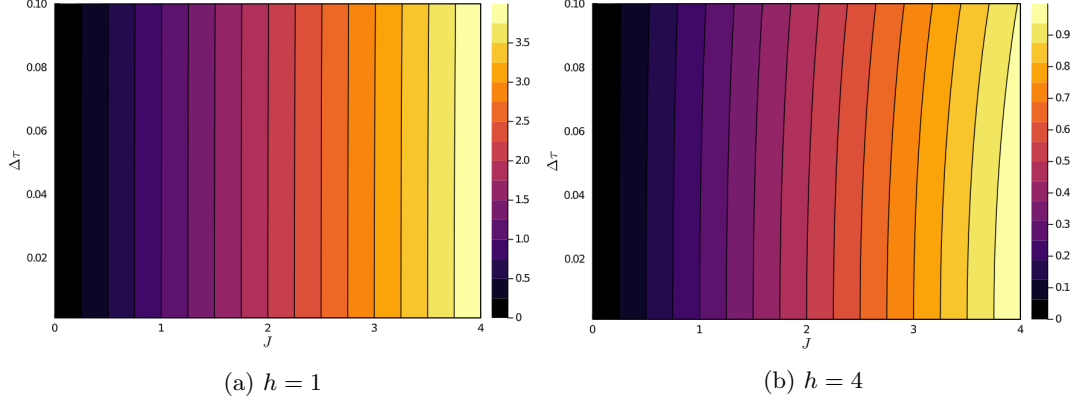


Figure 4: J_{xy}/J_τ under different h . It can be seen that (17) is highly anisotropic for a large range of J . Contour lines in (a) are straight, indicating that the discrete path integral works well even with large $\Delta\tau$, while contour lines in (b) are distorted, requiring us to use $\Delta\tau$ that is small enough.

$$\begin{aligned}
\langle \sigma^z(\tau + \Delta\tau) | e^{-\Delta\tau H} | \sigma^z(\tau) \rangle &= \langle \sigma^z(\tau + \Delta\tau) | e^{-\Delta\tau \sum_i h \sigma_i^x} e^{\Delta\tau \sum_{\langle i,j \rangle} J \sigma_i^z \sigma_j^z} | \sigma^z(\tau) \rangle \\
&= e^{\Delta\tau \sum_{\langle i,j \rangle} J \sigma_i^z \sigma_j^z} \langle \sigma^z(\tau + \Delta\tau) | e^{-\Delta\tau \sum_i h \sigma_i^x} | \sigma^z(\tau) \rangle \\
&= e^{\Delta\tau \sum_{\langle i,j \rangle} J \sigma_i^z \sigma_j^z} \sum_{\{\sigma_i^x\}} e^{-\Delta\tau \sum_i h \sigma_i^x} \langle \sigma^z(\tau + \Delta\tau) | \sigma^x \rangle \langle \sigma^x | \sigma^z(\tau) \rangle \\
&= e^{\Delta\tau \sum_{\langle i,j \rangle} J \sigma_i^z \sigma_j^z} \prod_i \sum_{\sigma_i^x} e^{-\Delta\tau h \sigma_i^x} \langle \sigma_i^z(\tau + \Delta\tau) | \sigma_i^x \rangle \langle \sigma_i^x | \sigma_i^z(\tau) \rangle \\
&= e^{\Delta\tau \sum_{\langle i,j \rangle} J \sigma_i^z \sigma_j^z} \prod_i \sum_{\sigma_i^x = \pm 1} e^{-\Delta\tau h \sigma_i^x} \frac{1}{2} e^{i\pi \frac{1-\sigma_i^x}{2} \left(\frac{1-\sigma_i^z(\tau)}{2} + \frac{1-\sigma_i^z(\tau+\Delta\tau)}{2} \right)} \\
&= \frac{1}{2^N} e^{\Delta\tau \sum_{\langle i,j \rangle} J \sigma_i^z \sigma_j^z} \prod_i \left(e^{-\Delta\tau h} + e^{\Delta\tau h} e^{i\pi \frac{1-\sigma_i^z(\tau)}{2}} e^{i\pi \frac{1-\sigma_i^z(\tau+\Delta\tau)}{2}} \right) \\
&= \frac{1}{2^N} e^{\Delta\tau \sum_{\langle i,j \rangle} J \sigma_i^z \sigma_j^z} \prod_i \left(e^{-\Delta\tau h} + e^{\Delta\tau h} \sigma_i^z(\tau) \sigma_i^z(\tau + \Delta\tau) \right).
\end{aligned}$$

And since $\sigma_i^z = \pm 1$, we have

$$\cosh J_\tau + \sinh J_\tau \sigma_i^z(\tau) \sigma_i^z(\tau + \Delta\tau) = e^{J_\tau \sigma_i^z(\tau) \sigma_i^z(\tau + \Delta\tau)},$$

so

$$e^{-\Delta\tau h} + e^{\Delta\tau h} \sigma_i^z(\tau) \sigma_i^z(\tau + \Delta\tau) \propto e^{J_\tau \sigma_i^z(\tau) \sigma_i^z(\tau + \Delta\tau)},$$

where

$$\tanh J_\tau = e^{2\Delta\tau h}.$$

So the discrete path integral of (16) with time step $\Delta\tau$ shares its weights with the partition function of the classical Ising model

$$H = -J_{xy} \sum_{\tau, \text{spacial } \langle i, j \rangle} \sigma_{i\tau} \sigma_{j\tau} - J_\tau \sum_{\tau, i} \sigma_{i\tau} \sigma_{i, \tau + \Delta\tau} \quad (17)$$

at $T = 1$, where

$$J_{xy} = \Delta\tau J, \quad \tanh J_\tau = e^{2\Delta\tau h}. \quad (18)$$

It should be noted that (17) may be highly anisotropic between time and space, which can be observed in Figure 4 on page 6. Another fact that can be read from Figure 4 on page 6 is that for large h $\Delta\tau$ should be smaller to keep the same accuracy. The larger h is, the stronger the quantum fluctuation is, and with strong quantum fluctuation $\Delta\tau$ must be small enough to accurately track the time evolution.

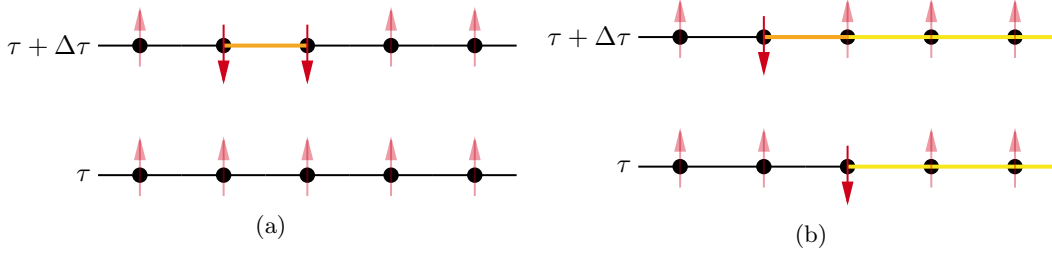


Figure 5: String fragments provided in (22). (a) corresponds to the $\sigma^+\sigma^+$ term, where a minimal string is created out of nothing, or in other words, two magnons are created out of nothing. (b) corresponds to the $\sigma^+\sigma^-$ term, which extends an existing string, or in other words, a magnon is moved to its nearest neighbor. The time inverse of (a) and (b) can be easily found, which are annihilation of a minimal string and shortening an existing string, correspondingly.

2.1.2 Cluster update algorithm along the temporal direction

The anisotropic feature of (17) is tackled in [1].

We did a benchmark of our algorithm with data provided in [3].

2.1.3 Worm Algorithm for 2D Transverse Field Ising Model

Another way to simulate 2D transverse field Ising model is described in [4]. We do the following (canonical) substitution

$$\sigma_i^x \longrightarrow -\sigma_i^z, \quad \sigma_i^z \longrightarrow -\sigma_i^x, \quad \sigma_i^y \longrightarrow -\sigma_i^y \quad (19)$$

in (16), and obtain

$$H = -J \sum_{\langle i,j \rangle} \sigma_i^x \sigma_j^x - h \sum_i \sigma_i^z. \quad (20)$$

which can be viewed as a string-net model, where the $\sum \sigma^z$ term is string tension term and the other term is the string kinetic term. The ends of a σ^z string are two sites on which $\sigma^z = -1$, as opposed to the “vacuum” case where $\sigma^z = 1$. We define the ladder operators in the standard way

$$\sigma_i^\pm = \frac{\sigma_i^x \pm i\sigma_i^y}{2}, \quad (21)$$

then (20) turns into

$$H = -J \sum_{\langle i,j \rangle} (\sigma_i^+ \sigma_j^- + \sigma_i^- \sigma_j^+ + \text{h.c.}) - h \sum_i \sigma_i^z, \quad (22)$$

which can also be rewrite into one of hardcore boson model.

The σ^z strings can expand and shrink, and their ends can hop from one site to its neighbors, according to the first four terms in the Hamiltonian, which are factories of string fragments. This is visualize in Figure 5 on page 7. It should be noted that the $\sigma^+\sigma^+$ term only applies to vacuum, or otherwise it just returns zero. Likewise, the $\sigma^+\sigma^-$ term only applies to existing strings, or otherwise it just returns zero. Two or more minimal strings can be created at the same time, so effectively, a prolonged string can be generated from vacuum in just one time step. As a result, the field configuration used in the path integral is something like this: a string is created, and then distorted, and finally annihilated. So each field configuration used in the path integral is a set of *closed* strings or loops, which are just *world lines* of magnons, as is depicted in Figure 6 on page 8. We name the $\sigma^+\sigma^+ + \text{h.c.}$ terms as **pairing**, the $\sigma^+\sigma^- + \text{h.c.}$ terms **hopping**.

Now we write down the partition function in the path integral form. Suppose there are m time steps. The discrete path integral is

$$Z = \sum_{\{\sigma_\tau\}} \langle \sigma_0 | e^{-\Delta\tau H} | \sigma_\beta \rangle \cdots \langle \sigma_{2\Delta\tau} | e^{-\Delta\tau H} | \sigma_{\Delta\tau} \rangle \langle \sigma_{\Delta\tau} | e^{-\Delta\tau H} | \sigma_0 \rangle \quad (23)$$

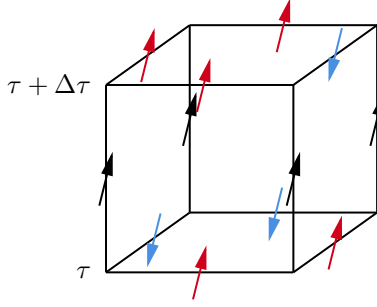


Figure 7: The temporal gauge: the red and blue spin degrees of freedom can rotate arbitrarily, while the black ones (which are on bonds with temporal directions) are fixed to 1.

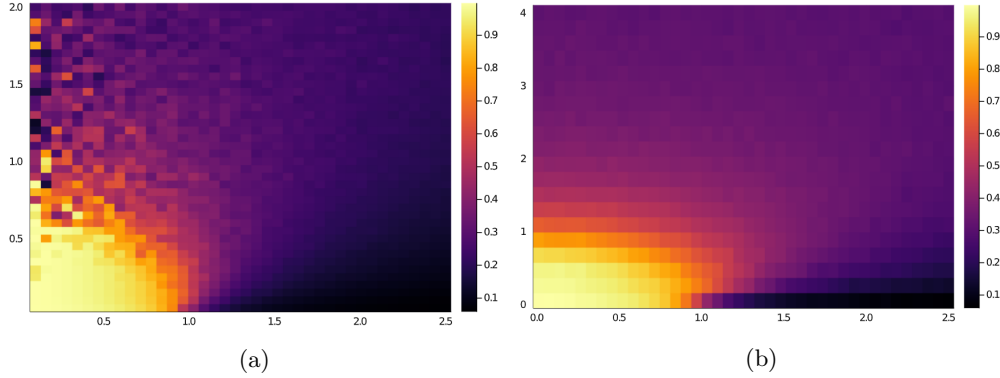


Figure 8: Phase diagrams of 1D transverse field Ising chain obtained with different updating algorithms. The x coordinate is h and the y coordinate is T . (a) Metropolis algorithm (b) Wolff cluster algorithm. It can be seen that Metropolis algorithm does not work well when h is small.

at $T = 1$. (25) actually does not have a \mathbb{Z}_2 gauge symmetry, as it can be seen as a 2+1 dimensional \mathbb{Z}_2 theory in the path integral formalism with gauge choice

$$\sigma_{i, \langle \tau, \tau + \Delta\tau \rangle} = 1, \quad (26)$$

shown in Figure 7 on page 9. This fact actually explains in an intuitively way why (8) does not work: by introducing a transverse field (or string tension term), we have already done an implicit gauge fixing with the form $\sigma = \dots$, and it is generally impossible to do another like (8).

3 Simulation of \mathbb{Z}_2 Gauge Theory with Different Approaches

3.1 Monte Carlo Simulation of the Pure \mathbb{Z}_2 Gauge Theory with Gauge (8)

3.1.1 The Phase Diagram

Since J_x and J_y differ a lot, Metropolis algorithm is incapable for the simulation of the anisotropic Ising model. Cluster update methods - in this project Wolff cluster updating [8] - must be used. Figure 8 on page 9 shows a comparison between Metropolis algorithm and Wolff algorithm, where Metropolis algorithm cannot update the system sufficiently when $h = 0$, since in that case the 2D classical Ising model corresponding to the 1D transverse field Ising chain degenerates into a classical 1D Ising chain due to the vanishing quantum fluctuation, so the coupling strength in the temporal direction approaches to infinite.

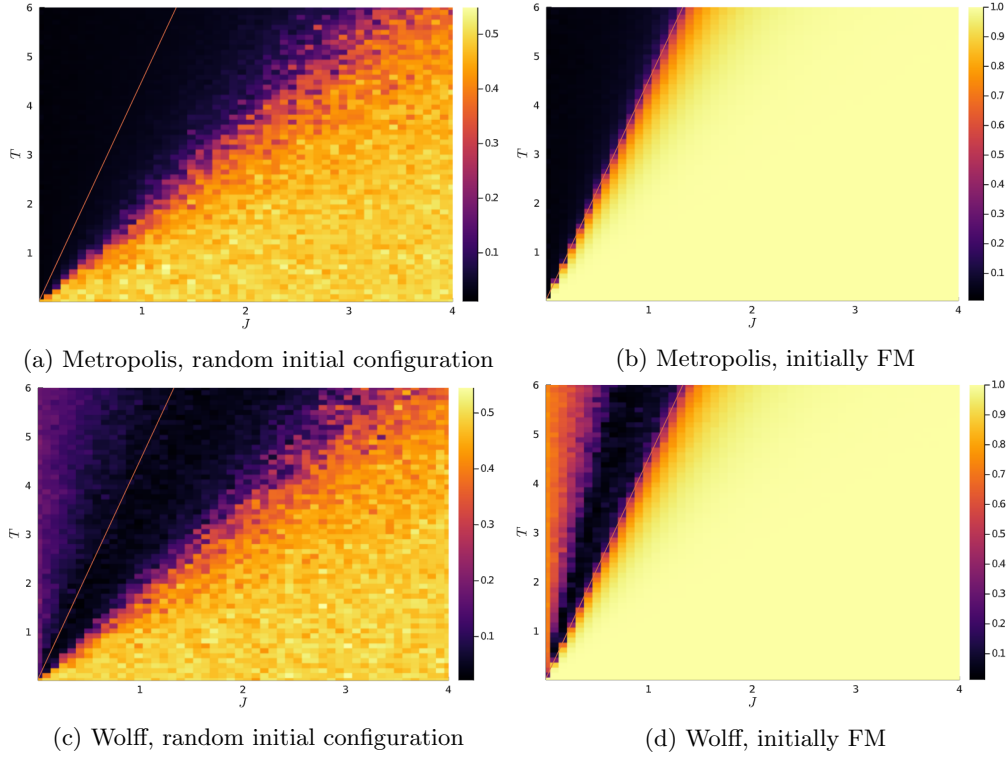


Figure 9: Simulation of 3D classical Ising model using Metropolis update and Wolff update. The data of the straight lines comes from [7].

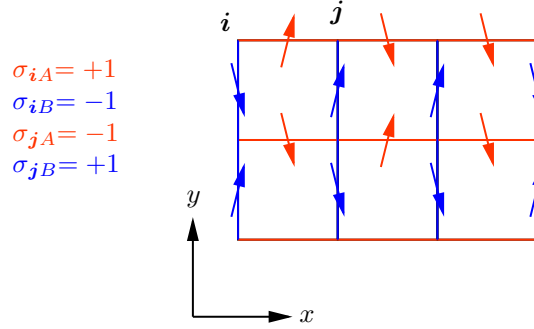


Figure 10: Dividing a gauge field configuration into two sublattices

3.2 Monte Carlo Simulation of the Pure \mathbb{Z}_2 Theory's Dual Transverse Field Ising Model

3.2.1 Benchmark of the Algorithms

Metropolis and Wolff update for Classical Ising Model

4 Monte Carlo Simulation of (1)

4.1 The \mathbb{Z}_2 Gauge Theory

\mathbb{Z}_2 gauge degrees of freedom are defined on bonds. Suppose there are N sites. Since there are 4 bonds connecting to one site and a bond is shared by two sites, there are $4N/2 = 2N$ bonds. Therefore, the \mathbb{Z}_2 gauge degrees of freedom can be divided into two sublattices, each of which has N degrees of freedom, shown in Figure 10 on page 10. Actually in order to be consistent with Julia's array indexing convention, we choose Figure 11 on page 11 as our convention to label the \mathbb{Z}_2 gauge degrees of freedom. Note that the definition of A sublattice and B sublattice

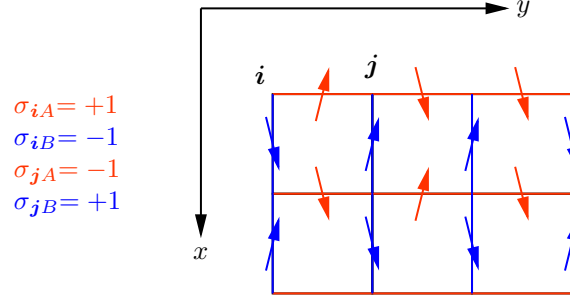


Figure 11: Another way to divide a gauge field configuration into two sublattices, in agreement with Julia’s index convention, where \mathbf{i} in $\dots[\mathbf{i}, \mathbf{j}]$ means x and \mathbf{j} means y .

in Figure 10 on page 10 is exactly opposite to the definition in Figure 11 on page 11.

4.2 Fermions

The way to update fermions can be found in the appendix of [2].

References

- [1] Henk W. J. Blöte and Youjin Deng. Cluster monte carlo simulation of the transverse ising model. *Physical Review E*, 66(6), December 2002.
- [2] Chuang Chen, Tian Yuan, Yang Qi, and Zi Yang Meng. Fermi arcs and pseudogap in a lattice model of a doped orthogonal metal. *Physical Review B*, 103(16), Apr 2021.
- [3] Zvi Friedman. Ising model with a transverse field in two dimensions: Phase diagram and critical properties from a real-space renormalization group. *Physical Review B*, 17(3):1429–1432, feb 1978.
- [4] Chun-Jiong Huang, Longxiang Liu, Yi Jiang, and Youjin Deng. Worm-algorithm-type simulation of the quantum transverse-field ising model. *Physical Review B*, 102(9), Sep 2020.
- [5] Eun-Gook Moon. Deconfined thermal phase transitions with \mathbb{Z}_2 gauge structures, 2019.
- [6] Rahul Nandkishore, Max A. Metlitski, and T. Senthil. Orthogonal metals: The simplest non-fermi liquids. *Physical Review B*, 86(4), Jul 2012.
- [7] A L Talapov and H W J Blöte. The magnetization of the 3d ising model. *Journal of Physics A: Mathematical and General*, 29(17):5727–5733, Sep 1996.
- [8] Ulli Wolff. Collective monte carlo updating for spin systems. *Physical Review Letters*, 62(4):361–364, Jan 1989.